Carcinogenesis vol.35 no.1 pp.131–137, 2014
doi:10.1093/carcin/bgt269
Advance Access publication August 28, 2013

Role of CYP2A13 in the bioactivation and lung tumorigenicity of the tobacco-specific lung procarcinogen 4-(methylnitrosamino)-1-(3-pyridyl)-1-butanone: *in vivo* studies using a CYP2A13-humanized mouse model

Vandana Megaraj, Xin Zhou, Fang Xie, Zhihua Liu, Weizhu Yang and Xinxin Ding*

Wadsworth Center, New York State Department of Health, and School of Public Health, State University of New York at Albany, Empire State Plaza, Box 509, Albany, NY 12201-0509, USA

*To whom correspondence should be addressed. Tel: +1 518 486 2585; Fax: +1 518 473 8722;
Email: xding@wadsworth.org

The tobacco-specific nitrosamine 4-(methylnitrosamino)-1-(3-pyridyl)-1-butanone (NNK), which is abundant in tobacco smoke, is a potent lung procarcinogen. The present study was aimed to prove that transgenic expression of human cytochrome P450 2A13 (CYP2A13), known to be selectively expressed in the respiratory tract and be the most efficient enzyme for NNK bioactivation *in vitro*, will enhance NNK bioactivation and NNK-induced tumorigenesis in the mouse lung. Kinetic parameters of NNK bioactivation *in vitro* and incidence of NNK-induced lung tumors *in vivo* were determined for wild-type, *Cyp2a5*-null and CYP2A13-humanized (CYP2A13-transgenic/*Cyp2a5*-null) mice. As expected, in both liver and lung microsomes, the loss of CYP2A5 resulted in significant increases in Michaelis constant (K_m) values for the formation of 4-oxo-4-(3-pyridyl)-butanal, representing the reactive intermediate that can lead to the formation of O^6-methylguanine (O^6-mG) DNA adducts; however, the gain of CYP2A13 at a fraction of the level of mouse lung CYP2A5 led to recovery of the activity in the lung, but not in the liver. The levels of O^6-mG, the DNA adduct highly correlated with lung tumorigenesis, were significantly higher in the lungs of CYP2A13-humanized mice than in *Cyp2a5*-null mice. Moreover, incidences of lung tumorigenesis were significantly greater in CYP2A13-humanized mice than in *Cyp2a5*-null mice, and the magnitude of the differences in incidence was greater at low (30 mg/kg) than at high (200 mg/kg) NNK doses. These results indicate that CYP2A13 is a low K_m enzyme in catalyzing NNK bioactivation *in vivo* and support the notion that genetic polymorphisms of CYP2A13 can influence the risks of tobacco-induced lung tumorigenesis in humans.

Introduction

Pulmonary cytochrome P450 (P450)-mediated metabolic activation of various environmental chemicals can lead to lung toxicity and carcinogenicity. Various P450 enzymes have been detected in human lungs (1), which are constantly challenged by exposures to airborne xenobiotics. One commonly occurring source of such exposures is cigarette smoke, which contains numerous chemicals that are known to cause lung cancer. Among them, 4-(methylnitrosamino)-1-(3-pyridyl)-1-butanone (NNK) is one of the most abundant and most potent nitrosamine; NNK induces lung adenocarcinomas in laboratory animals (2–4) and is classified as a human lung carcinogen (5).

NNK-induced lung tumorigenesis depends on P450-mediated metabolic activation in the target organ, the lung (2,6). NNK bioactivation by P450 enzymes leads to α-hydroxylation of the methyl or methylene carbon, yielding reactive electrophiles that can pyridyloxobutylate and methylate DNA, respectively, as well as stable metabolites that are detectable *in vitro*, including a keto alcohol, 4-hydroxy-1-(3-pyridyl)-1-butanone (HPB), and a keto aldehyde, 4-oxo-4-(3-pyridyl)-butanal (OPB). NNK is detoxified via either P450-mediated formation NNK-N-oxide or glucuronidation of its reduced form, 4-(methylnitrosamino)-1-(3-pyridyl)-1-butanol (NNAL) (2). Of the DNA adducts formed by NNK, including O^6-methylguanine (O^6-mG), 7-methylguanine, O^4-methylthymine, from the α-methylene hydroxylation pathway, and the HPB-releasing adducts, from the α-methyl hydroxylation pathway, O^6-mG is the most persistent and is the critical determinant of NNK-induced lung tumorigenesis in A/J mice (7). The HPB-releasing adducts also play an important role, by competing with O^6-mG for O^6-alkylguanine-DNA-alkyltransferase, thus inhibiting the repair of O^6-mG (8).

Multiple human P450 enzymes, including CYP1A, 2A, 2B, 2D and 3A, are capable of bioactivating NNK *in vitro* (2,9,10). However, strong evidence suggests that CYP2A13 may play a critical role in NNK bioactivation in the lung *in vivo*. CYP2A13 is expressed selectively in the respiratory tract and is the most efficient P450 in NNK bioactivation *in vitro* (9,11). Levels of CYP2A13 protein expression correlated with rates of microsomal NNK metabolic activation in human lungs (12). The *CYP2A13*2* allele, which causes decreased gene expression as well as lower enzyme activity toward NNK (13–15), was found to be associated with decreased incidences of lung adenocarcinoma in light smokers (16,17). Nonetheless, direct proof for the ability of human CYP2A13 to mediate NNK bioactivation and lung tumorigenesis *in vivo* has not been reported.

In the present study, we have performed NNK lung tumor bioassays in a CYP2A13-humanized mouse model. The CYP2A13-humanized mouse is a hybrid between *Cyp2a5*-null mouse (18) and CYP2A13-transgenic mouse (19), the latter harbors five copies (in hemizygotes) of the human *CYP2A13* gene (together with its neighboring *CYP2F1* and *CYP2B6* genes) contained in a bacterial artificial chromosome clone. Our recent studies have confirmed that mouse CYP2A5 plays a major role in NNK bioactivation in mouse lung (20) and that the transgenic CYP2A13 is functional in NNK bioactivation, both *in vitro* and *in vivo* (19). The aim of this study was to further determine the abilities of both CYP2A5 and CYP2A13 in NNK-induced lung tumorigenesis.

The *Cyp2a5*-null and CYP2A13-humanized mice were originally produced on a B6 genetic background. For lung tumor bioassays, we first converted their genetic background to that of A/J, a sensitive strain for NNK-induced lung tumorigenesis (4). Subsequent studies were performed in three mouse strains, wild-type (WT), *Cyp2a5*-null and CYP2A13-humanized, all on A/J background. Lung tumors were induced in the mice by a single intraperitoneal (i.p.) injection of NNK (4); multiple NNK doses were used to identify the lowest NNK dose capable of inducing lung tumor in the CYP2A13-humanized mice and to allow comparisons of dose–response curves among the strains. As controls, we also studied the enzyme kinetics of *in vitro* bioactivation of NNK and levels of *in vivo* O^6-mG adduct formation in lung and liver, as well as rates of systemic clearance of NNK and NNAL, in the three strains of mice. Our results offer direct evidence in support of the hypothesis that human CYP2A13 plays an essential role in NNK-induced lung carcinogenesis by acting as a low Michaelis constant (K_m) enzyme in NNK bioactivation in the target tissue, and the notion that expression of functional CYP2A13 in the lung is a risk factor for lung carcinogenesis in human smokers.

Abbreviations: CYP2A13, cytochrome P450 2A13; HPB, 4-hydroxy-1-(3-pyridyl)-1-butanone; i.p., intraperitoneal; K_m, Michaelis constant; NNAL, 4-(methylnitrosamino)-1-(3-pyridyl)-1-butanol; NNK, 4-(methylnitrosamino)-1-(3-pyridyl)-1-butanone; O^6-mG, O^6-methylguanine; OPB, 4-oxo-4-(3-pyridyl)-butanal; WT, wild-type.

Materials and methods

Chemicals and reagents

The sources of NNK, NNAL, 4-(methylnitrosamino)-1-(3-[2,4,5,6-D_4]-pyridyl)-1-butanone (D_4-NNK), 4-(methylnitrosamino)-1-(3-[2,4,5,6-D_4]-pyridyl)-1-

butanol (D_4-NNAL), O^6-mG, O^6-methyl-deoxyguanosine (O^6-Me-dG) and O^6-trideuteriomethyl-deoxyguanosine (O^6-CD3-dG) were the same as described previously (6). All solvents (acetonitrile, methanol and water) were of high-performance liquid chromatography grade (ThermoFisher Scientific, Waltham, MA).

Mouse breeding

The *Cyp2a5*-null mice (20) and *CYP2A13*-transgenic mice (19), both on C57BL/6 (B6) background, were obtained from breeding stocks maintained at the Wadsworth Center. *Cyp2a5*-null mice were backcrossed to A/J-WT mice for five generations (over a period of ~15 months), to obtain A/J-N_5-*Cyp2a5*$^{+/-}$ mice, which were then intercrossed to obtain A/J-N_5-*Cyp2a5*$^{-/-}$ mice. Hemizygous CYP2A13-transgenic mice on B6 background were crossbred with *Cyp2a5*-null mice on B6, yielding *CYP2A13*$^{+/-}$/*Cyp2a5*$^{+/-}$ pups, which were identified by genotyping. B6-*CYP2A13*$^{+/-}$/*Cyp2a5*$^{+/-}$ mice were also backcrossed to A/J-WT mice for five generations (over a period of ~15 months), to obtain A/J-N_5-*CYP2A13*$^{+/-}$/*Cyp2a5*$^{+/-}$ mice. The latter was crossbred with A/J-N_5-*Cyp2a5*-null mice to obtain A/J-N_5-*CYP2A13*$^{+/-}$/*Cyp2a5*$^{-/-}$ mice, which is also designated as A/J-N_5-CYP2A13-humanized mice (hemizygous for the *CYP2A13* transgene).

B6-*CYP2A13*$^{+/-}$/*Cyp2a5*$^{+/-}$ mice were also crossbred with B6-*Cyp2a5*$^{-/-}$ mice to obtain B6-CYP2A13-humanized mice. The latter, together with B6-*Cyp2a5*-null, B6 WT and A/J-WT mice, were used for studying NNK metabolism in the early phase of the project. A/J-WT and B6-WT mice were produced from breeding pairs maintained at the Wadsworth Center.

Mice were genotyped using tail DNA for the *Cyp2a5*$^-$ and *Cyp2a5*$^+$ alleles using primers F1 (5′-gccctacatcccccatatct-3′) and R1 (5′-acttgtgaggggtgttgg-3′), which yield a ~500-bp product from the *Cyp2a5*$^-$ allele and a ~3000-bp product (corresponding to a region spanning intron 7 and exon 9) from the *Cyp2a5*$^+$ allele. Mice were further genotyped for *CYP2A13* using primers F2 (5′-cctggacagatgcctttaactccg-3′) and R2 (5′-tggctttgcacctgcctgcact-3′), which yield a 332-bp product (corresponding to *CYP2A13* exon 5) (15). Mice positive for *Cyp2a5*$^-$ and *CYP2A13*, but negative for *Cyp2a5*$^+$, were identified as CYP2A13-humanized mice. Littermates that were positive for *Cyp2a5*$^-$, but negative for both *Cyp2a5*$^+$ and *CYP2A13*, were identified as *Cyp2a5*-null mice and used in the study.

Animal studies

All procedures involving animals were approved by the Institutional Animal Care and Use Committee of the Wadsworth Center. For pharmacokinetics study and determination of tissue levels of O^6-mG, 2-month-old A/J-WT, A/J-N5-*Cyp2a5*-null and A/J-N5-CYP2A13-humanized female mice were treated with a single injection of NNK (at 200, 100 or 30 mg/kg, i.p.) in saline. Blood samples (~20 µl each) from individual mice were collected from the tail at various time points (10 min to 4 h) after the injection. The samples were centrifuged at 1000*g*, for 5 min, at 4°C, for preparation of plasma. For studies on DNA adduct formation, liver and lung were obtained 4 h after NNK treatment. For determination of plasma NNK/NNAL and tissue O^6-mG levels, the samples were prepared for liquid chromatography-mass spectrometry analysis essentially as described previously (6). Female mice are studied in all experiments, to be consistent with NNK tumor bioassays, for which female mice are preferred (21).

Lung tumor bioassay was performed as described previously (22). Two-month-old A/J-WT, A/J-N_5-*Cyp2a5*-null and A/J-N5-CYP2A13-humanized female mice were treated with a single 0.15-ml dose of either saline or NNK (200, 100, 50 or 30 mg/kg body weight, i.p.). Following treatment the animals were maintained on AIN-93G diet (Dyets) until they were killed 4 months later for tumor detection. Body weights were recorded weekly. Lung tumor multiplicity (average number of tumors per mouse) and frequency (percentage of mice with tumors) were determined independently by two researchers, and the average of the two analyses is reported.

For histological characterization of lung tumors, tissues from NNK-treated (100 mg/kg group) WT, *Cyp2a5*-null and CYP2A13-humanized mice (four mice/strain) were fixed in 10% buffered formalin and processed for histological examination at the Pathology Laboratory of the Wadsworth Center. The lung sections were stained with hematoxylin and eosin. Light microscopic examinations of the sections were performed to examine the morphology of tumors in different strains of mice using standard criteria (23).

Other methods

Plasma levels of NNK and NNAL were determined with a liquid chromatography-mass spectrometry method, as described recently (20). *In vitro* assays of NNK metabolism were performed as described (20), using reaction mixtures that contained 100 mM potassium phosphate buffer, 0–200 µM NNK, 0.25 mg/ml liver or lung microsomal protein, 0 or 5 mM sodium bisulfite and 0 or 1.0 mM NADPH, in a final volume of 0.2 ml. Reactions were carried out at 37°C for up to 30 min and were terminated by the addition of 0.2 ml of acetonitrile. The rates of formation of the ketoaldehyde (OPB), keto alcohol (HPB) and NNK-N-oxide were determined using liquid chromatography-tandem mass spectrometry.

Tissue levels of O^6-mG were determined as described previously (6), with minor modifications. Briefly, genomic DNA samples (100–200 µg) were fortified with the internal standard O^6-CD3-dG (6 pmol) and hydrolyzed in 0.1 N HCl at 80°C for 90 min. The samples were allowed to cool, neutralized and then analyzed using liquid chromatography-mass spectrometry, as described elsewhere (20). Genomic DNA from tissues of saline-treated animals was used for preparation of calibration curves. Blank controls for solvent and matrix were included in each set of calibration samples. The detection limits for O^6-mG was 0.04 pmol (on column) with injection of 6 µg of hydrolyzed DNA. Levels of total guanine were determined using high-performance liquid chromatography, as described (6).

For data analysis, non-linear regression and enzyme kinetic analyses were performed using GraphPad Prism 5 (GraphPad, San Diego, CA). Student's *t*-test was used for comparisons between two groups. One-way analysis of variance was used for comparisons among three or more groups, followed by Dunnett's or Tukey's *post hoc* test for pairwise comparisons. Fisher's exact test was used for tumor frequency studies. In all cases, $P < 0.05$ was considered statistically significant.

Results

Role of CYP2A13 in the bioactivation of NNK in lung microsomes

Kinetic parameters for the formation of the three oxidative metabolites, NNK-N-oxide, HPB and OPB (detected as OPB-bisulfite), were determined for liver and lung microsomes from B6-WT, A/J-WT, B6-*Cyp2a5*-null and B6-CYP2A13-humanized female mice (Table I). Assays were performed using conditions under which the rates of

Table I. Apparent kinetic parameters for the formation of NNK metabolites by mouse lung and liver microsomes[a]

Metabolite		Lung				Liver			
		A/J-WT	B6-WT[b]	B6-*Cyp2a5*-null[b]	B6-CYP2A13-humanized	A/J-WT	B6-WT[b]	B6-*Cyp2a5*-null[b]	B6-CYP2A13-humanized
OPB	K_m (µM)	27.8±2.2	28.0±1.9	40.2±2.1[c]	28.2±2.3[d]	27±2	29±4	55±5[c]	55±4[c]
	V_{max} (pmol/min/mg)	58.1±2.3	57.3±1.8	61.5±2.0	57.2±2.1	220±10	220±10	210±10	210±8
	V_{max}/K_m	2.1±0.1	2.0±0.1	1.5±0.1[c]	2.0±0.1[d]	8.0±0.4	7.6±0.3	4.0±0.2[c]	4.0±0.2[c]
HPB	K_m (µM)	2.6±0.6	2.8±0.3	2.9±0.3	2.8±0.3	16±2	18±3	65±15[c]	67±15[c]
	V_{max} (pmol/min/mg)	24.5±1	24.3±0.5	24.4±1.0	25.0±0.6	102±3	105±5	70±8[c]	70±9[c]
	V_{max}/K_m	9.3±1.2	8.7±0.4	8.4±0.4	8.9±1.0	6.3±0.5	5.9±0.2	1.1±0.1[c]	1.0±0.1[c]
NNK-N-oxide	K_m (µM)	1.6±0.2	1.6±0.2	1.9±0.3	1.6±0.3	81±16	84±18	83±16	85±17
	V_{max} (pmol/min/mg)	37.1±1.8	35.8±3.1	38.7±2.2	35.2±2.0	19±2	19±2	20±2	20±2.0
	V_{max}/K_m	23.2±3.1	22.4±2.0	20.4±1.8	22.0±2.0	0.2±0	0.2±0	0.2±0	0.2±0

[a]Rates of microsomal metabolite formation, determined in 2-month-old female mice, were used for calculation of apparent kinetic parameters. Values represent means ± SD for data obtained from three different microsomal preparations per group.
[b]Data for B6-WT and B6-*Cyp2a5*-null mice (20) are included for comparison.
[c]$P < 0.01$ compared with A/J-WT and B6-WT mice (*t*-test).
[d]$P < 0.01$ compared with B6-*Cyp2a5*-null mice (*t*-test).

product formation were linear with time. Results for B6-*Cyp2a5*-null and B6-WT mice have been published as a part of another study (20). The values for the formation of OPB, HPB and NNK-N-oxide by lung microsomes were similar between A/J-WT and B6-WT mice; this result supports the relevance of the metabolic data, obtained from mice on B6 background, and the later tumorigenesis data, obtained from mice on A/J background.

As we have reported (20), the apparent K_m value for OPB formation by lung microsomes from *Cyp2a5*-null mice was significantly higher than that for WT mice, confirming the loss of the low K_m component (i.e. CYP2A5); however, the apparent K_m value for OPB formation by lung microsomes from CYP2A13-humanized mice was similar to that for WT mice, indicating gain of a low K_m enzyme. This result showed that, in lung microsomes, CYP2A13 (like CYP2A5) is a low K_m enzyme in the formation of OPB, which represents the α-hydroxylation pathway that leads to O^6-mG DNA adduct formation (2,8).

The apparent V_{max} values for OPB formation were not significantly different among the strains tested (Table I), probably reflecting contributions by other mouse P450s to NNK metabolism at higher substrate concentrations. The apparent K_m and V_{max} values for the formation of HPB and NNK-N-oxide by lung microsomes were also similar among the strains tested. Therefore, although CYP2A13 was efficient in catalyzing the formation of HPB (9), it did not play an important role in the formation of HPB (or NNK-N-oxide) in mouse lung microsomes.

In contrast to the results for lung microsomes, and consistent with the absence of significant CYP2A13 expression in the liver of the *CYP2A13*-transgenic mice (19), the apparent K_m values for the formation of OPB by liver microsomes were not different between *Cyp2a5*-null and CYP2A13-humanized mice (Table I). The kinetic parameters for the formation of HPB by liver microsomes were also not different between the null and the humanized mice. However, higher K_m values were observed for both OPB and HPB formation by liver microsomes from the null mice, compared with WT mice, indicating potential role of CYP2A5 in hepatic NNK bioactivation (20). Notably, the kinetic parameters for the formation of OPB and HPB by liver microsomes from A/J-WT mice were similar to previously reported values (7,24).

Systemic clearance of NNK and NNAL in A/J-WT, A/J-N5-Cyp2a5-null and A/J-N5-CYP2A13-humanized mice

To confirm that the expression of the human P450 transgenes do not alter the systemic elimination of NNK and its major circulating metabolite NNAL, plasma levels of NNK and NNAL were compared among the three mouse strains, at the lowest (30 mg/kg; Figure 1A) and the highest (200 mg/kg; Figure 1B) NNK doses to be used for tumor bioassays. As was previously reported for B6 mice (20), the present data for A/J mice showed that clearance of NNK or NNAL was not impacted by the loss of CYP2A5. Similarly, the gain of CYP2A13 did not change NNK and NNAL pharmacokinetics, at either of the NNK doses tested. The results indicate that lung CYP2A13 does not contribute to the systemic clearance of NNK or NNAL and document that the bioavailability of NNK was not different in the three mouse strains to be tested for lung tumorigenesis.

Role of CYP2A13 in the formation of O^6-mG

The role of CYP2A13 in NNK bioactivation *in vivo* was determined by measuring NNK-induced formation of O^6-mG DNA adduct in the lung, which is known to correlate with extent of NNK-induced lung tumorigenesis in A/J mice (7). O^6-mG levels in the lungs and livers of A/J-WT, A/J-N5-*Cyp2a5*-null and A/J-N5-CYP2A13-humanized mice (Table II) were determined at 4 h after NNK treatment, as described previously (20). As was reported for B6 mice (20), the loss

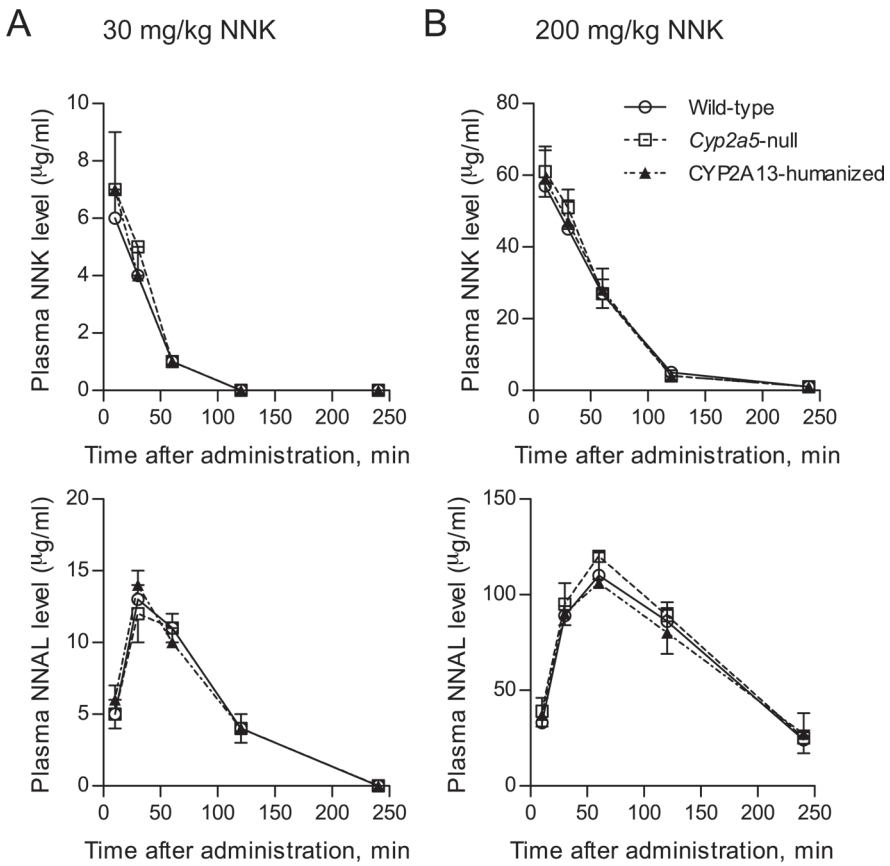

Fig. 1. Systemic levels of NNK and NNAL at various time points after i.p. administration of NNK. A/J-WT, A/J-N5-*Cyp2a5*-null and A/J-N5-CYP2A13-humanized mice (2-month-old, female) were injected with NNK at either 30 mg/kg (**A**) or 200 mg/kg (**B**), i.p., and plasma levels of NNK and NNAL were determined. Data represent means ± SD ($n = 4$). No significant difference was found among the three strains, at any time point, for either NNK or NNAL (Student's *t*-test).

Table II. NNK-induced O^6-mG adduct formation in the lung and liver[a]

NNK dose (mg/kg)	Strain	O^6-mG level (pmol/μmol guanine)	
		Lung	Liver
200	A/J-WT	37.0 ± 7.0	545 ± 46
	AJ-N5-*Cyp2a5*-null	28.3 ± 3.9	601 ± 36
	AJ-N5-CYP2A13-humanized	38.5 ± 7.2	608 ± 112
100	A/J-WT	28.9 ± 2.7	419 ± 44
	AJ-N5-*Cyp2a5*-null	20.2 ± 1.6[b]	406 ± 63
	AJ-N5-CYP2A13-humanized	28.0 ± 2.0	440 ± 33
30	A/J-WT	11.6 ± 2.0	130 ± 20
	AJ-N5-*Cyp2a5*-null	6.1 ± 0.9[b]	154 ± 28
	AJ-N5-CYP2A13-humanized	12.4 ± 1.1	144 ± 18

[a]Mice (female, 2-month-old) were injected with NNK at the indicated dose (i.p.), and levels of O^6-mG and total guanine were determined at 4 h after the injection. Data represent means ± SD ($n = 8$).
[b]$P < 0.05$, compared with A/J-WT and A/J-N5-CYP2A13-humanized mice (*t*-test).

of CYP2A5 also led to decreases in lung O^6-mG levels in the A/J mice, and the extent of decrease was dependent on NNK dose, ranging from 24% at 200 mg/kg to 47% at 30 mg/kg. The presence of CYP2A13 in the CYP2A13-humanized mice led to significant increases in O^6-mG levels, to levels that were comparable with those in A/J-WT mice. This result further confirms that CYP2A13, like CYP2A5, is a low K_m enzyme for NNK bioactivation in the mouse lung *in vivo*.

In the liver, the levels of O^6-mG were much higher than in the lung, but there was no significant difference in the adduct levels among the three mouse strains. This result contrasts with the *in vitro* activity data, which showed increased apparent K_m values for OPB formation in liver microsomes from the *Cyp2a5*-null mice (Table I). Thus, neither CYP2A5 nor CYP2A13 contributes to NNK bioactivation in liver *in vivo*, in the transgenic mouse model.

Role of CYP2A5 and CYP2A13 in NNK-induced lung tumorigenesis

To demonstrate the role of CYP2A13 as well as CYP2A5 in NNK-induced lung tumorigenesis, tumor bioassays were performed in A/J-WT, A/J-N5-*Cyp2a5*-null and A/J-N5-CYP2A13-humanized female mice. A standard protocol for NNK lung tumor bioassay was followed (4), with NNK given as a single i.p. injection at various doses (30–200 mg/kg), or with saline alone, and animals were killed 16 weeks after NNK treatment for counting tumors. As shown in Figure 2A, all mice exhibited continued weight gain during the assay period, irrespective of the strain, though the highest (200 mg/kg) NNK dose caused a significant decline in body weight, compared with the saline group. Notably, for each NNK dose and time point, mice of the three different strains were identical in body weight throughout the experimental period, as shown in Figure 2B for the 200 mg/kg dose groups. Additionally, at the time of necropsy (week 24), no treatment-related tumor or gross pathological changes was observed in the liver, heart, kidney, stomach or intestine of any of the mice studied (data not shown).

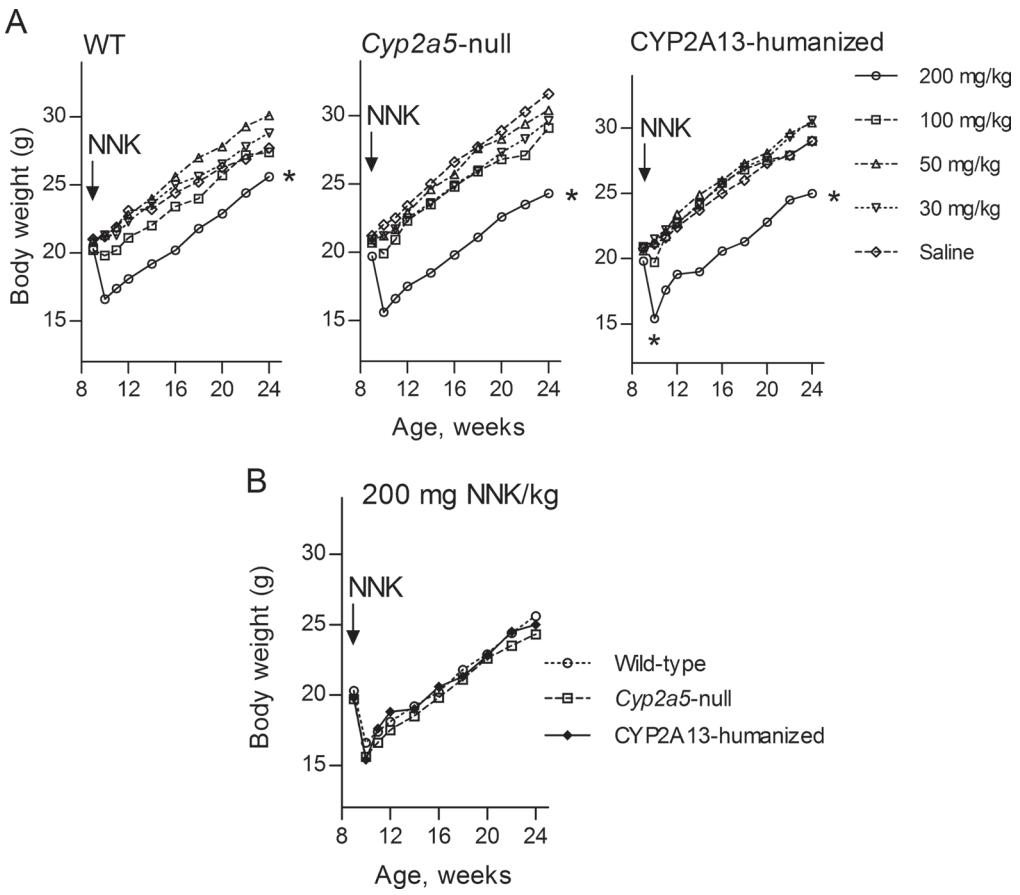

Fig. 2. Body weights of mice during NNK tumorigenesis study. A/J-WT, A/J-N5-*Cyp2a5*-null and A/J-N5-CYP2A13-humanized female mice were treated with single injection (i.p.) of NNK at the indicated dose or with saline at the beginning of the ninth week of age. Body weights were recorded at weekly intervals for a batch of 10 mice per group. The results shown are mean values, with standard deviation (data not shown) smaller than 10% of the mean. (**A**) Comparisons of weekly body weights among the treatment groups for each strain. *$P < 0.05$, compared with the saline group (one-way analysis of variance followed by Dunnett's test). (**B**) Comparisons of weekly body weights among the three different strains for the 200 mg/kg NNK dose ($P > 0.05$; one-way analysis of variance followed by Tukey's test).

Table III. NNK-induced lung tumorigenesis[a]

NNK dose (mg/kg)	Strain	Lung tumor multiplicity (tumors/mouse)	Lung tumor frequency (%)
200	A/J-WT	36.1 ± 2.1	100
	AJ-N5-*Cyp2a5*-null	23.1 ± 1.0[b]	100
	AJ-N5-CYP2A13-humanized	34.4 ± 1.0	100
100	A/J-WT	24.5 ± 1.1	100
	AJ-N5-*Cyp2a5*-null	15.1 ± 0.9[b]	100
	AJ-N5-CYP2A13-humanized	22.0 ± 1.0	100
50	A/J-WT	14.5 ± 1.2	100
	AJ-N5-*Cyp2a5*-null	6.2 ± 0.8[b]	95
	AJ-N5-CYP2A13-humanized	13.1 ± 1.4	100
30	A/J-WT	4.0 ± 0.3	95
	AJ-N5-*Cyp2a5*-null	1.2 ± 0.2[b]	77
	AJ-N5-CYP2A13-humanized	4.4 ± 0.6	95
0 (saline)	A/J-WT	0.05 ± 0	4.5[c]
	AJ-N5-*Cyp2a5*-null	0	0[c]
	AJ-N5-CYP2A13-humanized	0.13 ± 0.07	9.1[c]

[a]Two-month-old female mice were treated with a single injection of saline or NNK at the indicated dose (i.p.). Thereafter, the mice were kept on AIN93G diet until they were killed for tumor detection, at 4 months after the NNK or saline injection. Tumor multiplicity is shown as mean ± standard error ($n = 22$). Tumor frequency was calculated as percentage of mice with tumor in each group.
[b]$P < 0.05$, compared with A/J-WT and A/J-N5-CYP2A13-humanized mice (one-way analysis of variance for each dose followed by Tukey's test).
[c]$P < 0.05$, compared with the NNK-treated groups (Fisher's exact test).

As expected, saline-treated mice had a low incidence of 'spontaneous' lung tumors (Table III). In NNK-treated mice, tumor frequency was 100% at the 200 and 100 mg/kg doses, and was decreased slightly (to 77–95%) at the lowest dose; but there was no significant difference in tumor frequency among the three strains, for either the saline group or any of the NNK dose groups (Table III). Histopathological analysis of the lung tumors detected indicated they are primarily adenomas (data not shown), consistent with previous reports (6,25).

The number of lung tumors observed per mouse increased in a dose-dependent fashion (Table III; Figure 3A). For all NNK doses tested, the loss of CYP2A5 in the *Cyp2a5*-null mice caused a significant decrease in tumor multiplicity, compared with WT mice. The magnitude of the decrease was the greatest at the lowest NNK dose (30 mg/kg), ~70%, compared with a 35% reduction at the 200 mg/kg NNK dose. Compared with the *Cyp2a5*-null mice, the gain of CYP2A13 in the CYP2A13-humanized mice led to significant increases in lung tumor multiplicity at all NNK doses tested. The extent of the increase was the greatest at the 30 mg/kg dose, almost 4-fold, compared with ~1.6-fold at the two highest NNK doses (Figure 3B). Indeed, the tumor multiplicity was not significantly different between WT and CYP2A13-humanized mice for all the NNK doses tested (Figure 3A). These results are consistent with differences among the three strains in levels of O^6-mG in the lung and provide strong evidence in support of the notion that mouse CYP2A5 and human CYP2A13 are both highly capable of initiating NNK-induced lung tumorigenesis.

Discussion

This is the first study to directly demonstrate a role of mouse CYP2A5, as well as human CYP2A13, in NNK-induced lung tumorigenesis. Previously, the role of CYP2A5 in NNK-induced lung tumorigenesis in mice was deduced on the basis of a strong inhibition of the tumorigenesis by 8-methoxypsoralen (26); however, a more recent study in *Cyp2a5*-null mice showed that the compound also inhibited NNK bioactivation by other P450 enzymes in mouse lung (20). The role of CYP2A5 was also implicated by the impact of a strain-specific *Cyp2a5* genetic polymorphism on NNK lung tumorigenesis (27). Notably, although our present data clearly indicate a role for CYP2A5 in NNK-induced lung tumorigenesis, significant numbers of lung tumors were detected in NNK-treated *Cyp2a5*-null mice, even at the lowest NNK dose studied. The occurrence of this residual NNK-induced tumorigenesis is consistent with our earlier report of considerable amounts of residual NNK bioactivation activity (20) and supports previous suggestions of contributions by additional mouse lung P450 enzymes, such as CYP2B, to NNK-induced lung tumorigenesis (2,20,28).

Given the known activity of CYP2A5 toward NNK (20,29,30), we expected that the presence of CYP2A5 will make it difficult to determine the contribution of CYP2A13 to NNK metabolism and tumorigenesis. Therefore, we compared CYP2A13-humanized mice with *Cyp2a5*-null mice, in order to deduce the specific role of CYP2A13 in NNK-induced lung tumorigenesis. The gain of CYP2A13 in the CYP2A13-humanized mice was associated with a dose-dependent increase in NNK-induced O^6-mG adduct formation in the lung, compared with *Cyp2a5*-null mice. The extent of increase was larger at the low NNK dose of 30 mg/kg (100%) than at the 100 mg/kg dose (40%).

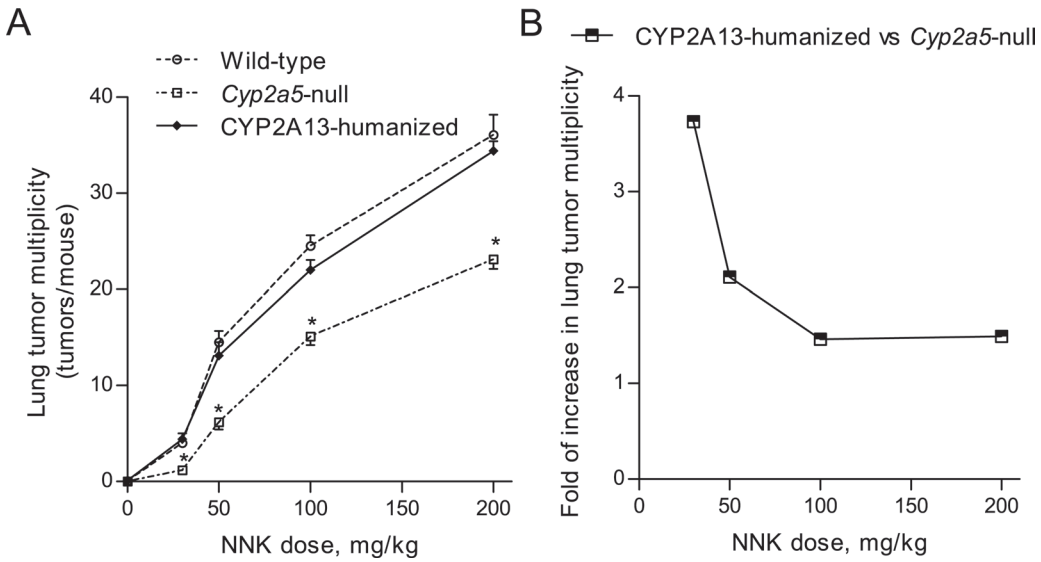

Fig. 3. Dose-response of NNK-induced lung tumorigenesis. (**A**) Tumor multiplicity data from Table III are plotted to show dose-dependent increase. Values represent means ± standard error ($n = 22$). *$P < 0.05$, compared with A/J-WT and A/J-N5-CYP2A13-humanized mice (one-way analysis of variance for each dose followed by Tukey's test). (**B**) Extent of increase (fold) in tumor multiplicity (mean values) in A/J-N5-CYP2A13-humanized mice, compared with A/J-*Cyp2a5*-null mice, at various NNK doses, showing greater contribution of CYP2A13 to lung tumorigenesis at the two lower doses tested.

This result, which is consistent with the *in vitro* data showing significantly lower apparent K_m values in the humanized mice than in the null mice for the formation of OPB, a marker for the reactive metabolite that leads to O^6-mG adduct formation, indicated that CYP2A13 is a low K_m enzyme (compared with remaining P450 enzymes in the *Cyp2a5*-null mice) for NNK bioactivation in lung, both *in vitro* and *in vivo*. This result is similar to our recent finding (as confirmed here) that CYP2A5 is a low K_m enzyme (compared with remaining P450 enzymes in the *Cyp2a5*-null mice) for NNK bioactivation in lung (20). In contrast, the contribution of CYP2A13 to O^6-mG adduct formation in the liver was negligible, consistent with its scant expression in that tissue (19). Notably, the low K_m status of CYP2A13 and CYP2A5 in NNK bioactivation in the lung is also reflected in the dose-dependent contributions of these enzymes to NNK-induced lung tumorigenesis. Although the lung tumor multiplicity was lower in *Cyp2a5*-null mice than in either WT or CYP2A13-humanized mice at all NNK doses tested, the magnitude of difference was greater at the low NNK dose of 30 mg/kg (~4-fold) than at the high NNK dose of 200 mg/kg (~1.5-fold).

A comparison of the DNA adduct data and the tumor bioassay data indicated that the influence of CYP2A13 (or CYP2A5) on tumorigenesis was more pronounced (in terms of change fold) than the influence on O^6-mG formation. This discrepancy might be explained by the threshold effect in NNK tumorigenesis. At the lowest NNK dose studied (30 mg/kg), lung tumors were detected in all three mouse strains; however, 23% of the *Cyp2a5*-null mice had no detectable tumors even though O^6-mG adduct formation was evident. This result supports the notion that DNA adducts below a certain threshold level can be efficiently repaired, e.g. by O^6-alkylguanine-DNA-alkyltransferase, and thus fail to initiate tumor formation (7). Therefore, the influence of CYP2A13/CYP2A5 on the levels of DNA adducts above the threshold level is more relevant to tumor outcome, and the change folds in adduct formation and in tumor multiplicity are actually more comparable.

A remarkable finding in this study is that, although the levels of CYP2A13 protein expression in the lungs of the humanized mouse model was ~50 times (hemizygotes) lower than the mouse lung CYP2A5 levels in WT mice (19), the contribution of CYP2A13 to NNK bioactivation and subsequent O^6-mG adduct formation and tumorigenesis in the humanized mice was comparable with the contribution of mouse CYP2A5 in WT mice. Given that these studies were performed in hemizygous CYP2A13-humanized mice, we expect to see even greater contributions from CYP2A13 in homozygous mice. The apparently much higher efficiency of CYP2A13 than CYP2A5 toward NNK bioactivation *in vivo* is consistent with results of previous *in vitro* enzyme kinetics studies using recombinant CYP2A13 and CYP2A5. Although the K_m values of CYP2A5 and CYP2A13 for OPB formation in reconstituted systems are similar (both ~4 μM) (9), the V_{max} value of CYP2A5 was much lower (~2 pmol/min/pmol P450) (9,22) than that of CYP2A13 (~14 pmol/min/pmol P450) (9,30) in this reaction, thus making CYP2A13 more efficient than CYP2A5.

The CYP2A13 protein level in lung microsomes of the CYP2A13-transgenic mice (19) was ~5-fold (for hemizygotes) higher than the highest level of CYP2A13 protein detected in human lung biopsy samples (12). We believe that the level present in the transgenic mouse lung is comparable with CYP2A13 levels in healthy human lungs, given the likely effects of postmortem degradation, oxidative stress associated with surgical procedures and systemic disease status, such as inflammation (31), on P450 expression. Additionally, the CYP2A13-humanized mouse utilized in this study harbored three human *CYP* transgenes, *CYP2A13*, *CYP2B6* and *CYP2F1*. However, the presence of *CYP2B6* and *CYP2F1* should not impact our conclusion on the role of CYP2A13 in mediating NNK-induced lung tumorigenesis, given the facts that CYP2B6 protein was not detected in lung microsomes of the transgenic mice (19) and that human CYP2F1 has very limited activity toward NNK (10). In the latter study, a recombinant human CYP2F1 was found to exhibit a rate of NNK metabolism much lower than that of CYP1A2, which itself was far less active than was CYP2A13 toward NNK (9). Therefore, the transgenic CYP2F1 is unlikely to make a noticeable contribution to NNK metabolic activation in the humanized mouse. In that connection, our preliminary study with lung microsomes from the *Cyp2f2*-null mice established that mouse CYP2F2 (the ortholog of CYP2F1) did not contribute to OPB formation in mouse lung (data not shown).

In summary, our results strongly support the conclusion that human CYP2A13 is efficient in NNK bioactivation *in vivo* and it can mediate NNK-induced lung tumorigenesis at relatively low NNK doses and at enzyme levels expected to be present in healthy human lungs. Tobacco smoke contains many toxic chemicals, and metabolic activation of tobacco-related procarcinogens undoubtedly involves multiple enzymes and pathways. A single enzyme can hardly account for all of the toxicity of cigarette smoking; therefore, an individual with deficient CYP2A13 expression or activity is not necessarily protected against smoking-induced lung tumorigenesis, given the potential roles of other enzymes and additional carcinogens. Nonetheless, our study provides proof-of-principle that individuals with relatively high expression of functional CYP2A13 are at greater risks of developing cigarette smoke-induced lung cancer. Furthermore, the demonstration of CYP2A13-mediated lung tumorigenesis in a mouse model also makes this model valuable for directly testing the efficacy of chemoprevention agents that target CYP2A13 for inhibition.

Funding

National Cancer Institute; National Institutes of Health (CA092596 to X.D.).

Acknowledgements

We thank Drs Q-Y.Zhang and R.Turesky of the Wadsworth Center for helpful discussions. We gratefully acknowledge the use of the Biochemistry, Molecular Genetics, Histopathology, and Advanced Light Microscopy and Image Analysis Core Facilities of the Wadsworth Center.

Conflict of Interest Statement: None declared.

References

1. Ding,X. *et al.* (2003) Human extrahepatic cytochromes P450: function in xenobiotic metabolism and tissue-selective chemical toxicity in the respiratory and gastrointestinal tracts. *Annu. Rev. Pharmacol. Toxicol.*, **43**, 149–173.
2. Hecht,S.S. (1998) Biochemistry, biology, and carcinogenicity of tobacco-specific N-nitrosamines. *Chem. Res. Toxicol.*, **11**, 559–603.
3. Hecht,S.S. *et al.* (1980) Comparative carcinogenicity in F344 rats of the tobacco-specific nitrosamines, N'-nitrosonornicotine and 4-(N-methyl-N-nitrosamino)-1-(3-pyridyl)-1-butanone. *Cancer Res.*, **40**, 298–302.
4. Hecht,S.S. *et al.* (1989) Rapid single-dose model for lung tumor induction in A/J mice by 4-(methylnitrosamino)-1-(3-pyridyl)-1-butanone and the effect of diet. *Carcinogenesis*, **10**, 1901–1904.
5. IARC (2007) Smokeless tobacco and some tobacco-specific N-nitrosamine. *IARC Monographs on the Evaluation of Carcinogenic Risks to Human*, Vol. **89**, International Agency for Research on Cancer, Lyon, pp. 421–589.
6. Weng,Y. *et al.* (2007) Determination of the role of target tissue metabolism in lung carcinogenesis using conditional cytochrome P450 reductase-null mice. *Cancer Res.*, **67**, 7825–7832.
7. Peterson,L.A. *et al.* (1991) O^6-methylguanine is a critical determinant of 4-(methylnitrosamino)-1-(3-pyridyl)-1-butanone tumorigenesis in A/J mouse lung. *Cancer Res.*, **51**, 5557–5564.
8. Peterson,L.A. *et al.* (1993) Pyridyloxobutyl DNA adducts inhibit the repair of O^6-methylguanine. *Cancer Res.*, **53**, 2780–2785.
9. Jalas,J.R. *et al.* (2005) Cytochrome P450 enzymes as catalysts of metabolism of 4-(methylnitrosamino)-1-(3-pyridyl)-1-butanone, a tobacco specific carcinogen. *Chem. Res. Toxicol.*, **18**, 95–110.
10. Smith,T.J. *et al.* (1992) Metabolism of 4-(methylnitrosamino)-1-(3-pyridyl)-1-butanone in human lung and liver microsomes and cytochromes P-450 expressed in hepatoma cells. *Cancer Res.*, **52**, 1757–1763.
11. Su,T. *et al.* (2000) Human cytochrome P450 CYP2A13: predominant expression in the respiratory tract and its high efficiency metabolic activation of a tobacco-specific carcinogen, 4-(methylnitrosamino)-1-(3-pyridyl)-1-butanone. *Cancer Res.*, **60**, 5074–5079.

12. Zhang,X. *et al.* (2007) CYP2A13: variable expression and role in human lung microsomal metabolic activation of the tobacco-specific carcinogen 4-(methylnitrosamino)-1-(3-pyridyl)-1-butanone. *J. Pharmacol. Exp. Ther*., **323**, 570–578.
13. D'Agostino,J. *et al.* (2008) Characterization of CYP2A13*2, a variant cytochrome P450 allele previously found to be associated with decreased incidences of lung adenocarcinoma in smokers. *Drug Metab. Dispos*., **36**, 2316–2323.
14. Schlicht,K.E. *et al.* (2007) Functional characterization of CYP2A13 polymorphisms. *Xenobiotica*., **37**, 1439–1449.
15. Zhang,X. *et al.* (2002) Genetic polymorphisms of the human CYP2A13 gene: identification of single-nucleotide polymorphisms and functional characterization of an Arg257Cys variant. *J. Pharmacol. Exp. Ther*., **302**, 416–423.
16. Kiyohara,C. *et al.* (2005) CYP2A13, CYP2A6, and the risk of lung adenocarcinoma in a Japanese population. *J. Health Sci*., **51**, 658–666.
17. Wang,H. *et al.* (2003) Substantial reduction in risk of lung adenocarcinoma associated with genetic polymorphism in CYP2A13, the most active cytochrome P450 for the metabolic activation of tobacco-specific carcinogen NNK. *Cancer Res*., **63**, 8057–8061.
18. Zhou,X. *et al.* (2010) Role of CYP2A5 in the clearance of nicotine and cotinine: insights from studies on a Cyp2a5-null mouse model. *J. Pharmacol. Exp. Ther*., **332**, 578–587.
19. Wei,Y. *et al.* (2012) Generation and characterization of a CYP2A13/2B6/2F1-transgenic mouse model. *Drug Metab. Dispos*., **40**, 1144–1150.
20. Zhou,X. *et al.* (2012) Role of CYP2A5 in the bioactivation of the lung carcinogen 4-(methylnitrosamino)-1-(3-pyridyl)-1-butanone in mice. *J. Pharmacol. Exp. Ther*., **341**, 233–241.
21. Anderson,L.M. *et al.* (1991) Tumorigenicity of the tobacco-specific carcinogen 4-(methyl-nitrosamino)-1-(3-pyridyl)-1-butanone in infant mice. *Cancer Lett*., **58**, 177–181.
22. Jalas,J.R. *et al.* (2003) Stereospecific deuterium substitution attenuates the tumorigenicity and metabolism of the tobacco-specific nitrosamine 4-(methylnitrosamino)-1-(3-pyridyl)-1-butanone (NNK). *Chem. Res. Toxicol*., **16**, 794–806.
23. Gordon,T. *et al.* (2009) Strain-dependent differences in susceptibility to lung cancer in inbred mice exposed to mainstream cigarette smoke. *Cancer Lett*., **275**, 213–220.
24. Nunes,M.G. *et al.* (1998) Inhibition of 4-(methylnitrosamino)-1-(3-pyridyl)-1-butanone (NNK) metabolism in human hepatic microsomes by ipomeanol analogs–an exploratory study. *Cancer Lett*., **129**, 131–138.
25. Belinsky,S.A. *et al.* (1992) Role of the alveolar type II cell in the development and progression of pulmonary tumors induced by 4-(methylnitrosamino)-1-(3-pyridyl)-1-butanone in the A/J mouse. *Cancer Res*., **52**, 3164–3173.
26. Miyazaki,M. *et al.* (2005) Mechanisms of chemopreventive effects of 8-methoxypsoralen against 4-(methylnitrosamino)-1-(3-pyridyl)-1-butanone-induced mouse lung adenomas. *Carcinogenesis*, **26**, 1947–1955.
27. Hollander,M.C. *et al.* (2011) A Cyp2a polymorphism predicts susceptibility to NNK-induced lung tumorigenesis in mice. *Carcinogenesis*, **32**, 1279–1284.
28. Smith,T.J. *et al.* (1993) Mechanisms of inhibition of 4-(methylnitrosamino)-1-(3-pyridyl)-1-butanone bioactivation in mouse by dietary phenethyl isothiocyanate. *Cancer Res*., **53**, 3276–3282.
29. Felicia,N.D. *et al.* (2000) Characterization of cytochrome P450 2A4 and 2A5-catalyzed 4-(methylnitrosamino)-1-(3-pyridyl)-1-butanone (NNK) metabolism. *Arch. Biochem. Biophys*., **384**, 418–424.
30. Jalas,J.R. *et al.* (2003) Comparative metabolism of the tobacco-specific nitrosamines 4-(methylnitrosamino)-1-(3-pyridyl)-1-butanone and 4-(methylnitrosamino)-1-(3-pyridyl)-1-butanol by rat cytochrome P450 2A3 and human cytochrome P450 2A13. *Drug Metab. Dispos*., **31**, 1199–1202.
31. Wu,H. *et al.* (2013) Transcriptional suppression of CYP2A13 expression by lipopolysaccharide in cultured human lung cells and the lungs of a CYP2A13-humanized mouse model. *Tox. Sci*., in press. doi:10.1093/toxsci/kft165.

Received April 19, 2013; revised July 18, 2013; accepted July 30, 2013